THEORETICAL ANALYSIS OF SEISMIC GROUND MOTIONS FOR A DIPPING LAYER

Y. Niwa (I)
S. Hirose (II)
Presenting Author: S. Hirose

SUMMARY

In this paper, the theoretical analysis of seismic ground motions, especially, concerning diffracted waves in a dipping layer is discussed. To this problem, the boundary integral equation (BIE) method is applied. The main advantage in the BIE formulation presented here is feasibility to solve the diffracted wave field, while it is known that the diffracted waves in a dipping layer can not be exactly evaluated by means of the ray theory (Refs. 1 and 2). By comparing results obtained by the BIE method with those of the ray theory, it is shown that the diffracted waves have much effect on seismic ground motions, and some numerical examples are presented.

INTRODUCTION

Various geological structures have been well known to affect seismic ground motions . In particular, horizontally varied geological structures, which consist of irregular surfaces and interfaces, give rise to locally distributed earthquake disasters. A dipping layer is one of such structures and it represents the model of continental boundary region, or sediment-filled vally and bed rock system.

Up to now, several numerical methods, such as FEM, FDM, Aki-Larner's method, and ray theory etc., have been developed to investigate the effect of complicated geological structures on seismic motions (Ref. 3). Concerning the reflected waves in a dipping layer, Ishii and Ellis (Refs. 1 and 2) proposed the ray theory to solve this problem by taking account of reflections of body waves. However, it is pointed out that no diffracted wave could be evaluated by means of their method.

In this paper, the boundary integral equation (BIE) method is employed to analyze the same problems as in Refs. 1 and 2, because the BIE method has analytical feasibility for wave propagation problems in a half space (Refs. 4 and 5). The BIE method presented here has the distinctive feature in respect that the BIE formulation is applied to the diffracted wave field only, not to total wave field(Refs. 4 and 5). In this case, computed results by the BIE method involve not only reflected waves but also diffracted waves. And they are compared with results obtained by the ray theory to clarify the effect of the diffracted waves on seismic ground motions.

STATEMENT OF THE PROBLEM

Fig. 1 shows the dipping layer model to be analyzed. The domains D^- and

(I) Professor of Civil Engineering, Kyoto University, Kyoto, JAPAN

(II) Instructor of Civil Engineering, Kyoto University, Kyoto, JAPAN

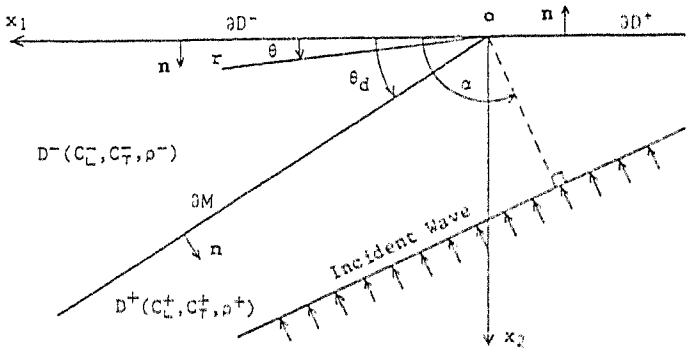

fig. 1 The dipping layer model to be analyzed.

D^+ denote a dipping layer and a bed rock, respectively. Both domains are isotropic, homogeneous, linear elastic, and in the plane strain state. The harmonic plane wave $\mathbf{u}^I$ is incident on the boundaries ∂M and ∂D^+ with an incident angle α. This problem reduces to the steady state two-dimensional one, then the governing equations become, in case of no body force

$$\mathbf{L}(C_L^-, C_T^-, \rho^-; \partial)\mathbf{u}(\mathbf{X},\omega)+\omega^2\mathbf{u}(\mathbf{X},\omega)=\mathbf{0} \quad \text{in } D^- \tag{1}$$

$$\mathbf{L}(C_L^+, C_T^+, \rho^+; \partial)\mathbf{u}(\mathbf{X},\omega)+\omega^2\mathbf{u}(\mathbf{X},\omega)=\mathbf{0} \quad \text{in } D^+ \tag{2}$$

where $\mathbf{L}$ is the differential operator defined as

$$\mathbf{L}(C_L, C_T, \rho; \partial) \equiv \begin{cases} \rho(C_T^2\nabla^2\mathbf{1}+(C_L^2-C_T^2)\nabla\nabla\cdot) & \text{for P-SV problems} \quad (3) \\ \rho C_T^2\nabla^2 & \text{for SH problems} \quad (4) \end{cases}$$

and $\mathbf{u}$, C_L, C_T, ρ and ω are displacement components, longitudinal wave velocity, transverse wave velosity, mass density, and angular frequency, respectively. Also note that the displacement components correspond to the following quantities,

$$\mathbf{u}=(u_1, u_2) \quad \text{for P-SV problems} \tag{5}$$

$$\mathbf{u}=u_3 \quad \text{for SH problems.} \tag{6}$$

The boundary conditions on ∂D^- and ∂D^+, and the continuity conditions on ∂M are prescribed in the following equations,

$$\mathbf{t}(\mathbf{x},\omega)\equiv\overset{n}{\mathbf{T}}(C_L, C_T, \rho; \partial)\mathbf{u}(\mathbf{x},\omega)=\mathbf{0} \quad \text{on } \partial D^- \text{ and } \partial D^+ \tag{7}$$

$$\lim_{\substack{\mathbf{X} \text{ in } D^- \\ \to \mathbf{x} \text{ on } \partial M}} \mathbf{u}(\mathbf{X},\omega)=\lim_{\substack{\mathbf{X} \text{ in } D^+ \\ \to \mathbf{x} \text{ on } \partial M}} \mathbf{u}(\mathbf{X},\omega) \quad \text{and} \quad \lim_{\substack{\mathbf{X} \text{ in } D^- \\ \to \mathbf{x} \text{ on } \partial M}} \mathbf{t}(\mathbf{X},\omega)=\lim_{\substack{\mathbf{X} \text{ in } D^+ \\ \to \mathbf{x} \text{ on } \partial M}} \mathbf{t}(\mathbf{X},\omega) \quad \text{on } \partial M \tag{8}$$

where

$$\overset{n}{\mathbf{T}}(C_L, C_T, \rho; \partial) \equiv \begin{cases} \rho((C_L^2-2C_T^2)\mathbf{n}\nabla\cdot+C_T^2(2(\mathbf{n}\cdot\nabla)\mathbf{1}+\mathbf{n}\times\nabla\times)) & \text{for P-SV problems} \quad (9) \\ \rho C_T^2\mathbf{n}\cdot\nabla & \text{for SH problems} \quad (10) \end{cases}$$

and $\mathbf{n}$ denotes a unit normal on each boundary as shown in Fig. 1.

RAY THEORY

The plane wave incident on the boundary ∂M reflects several times in the dipping layer D^- and then propagates downward without further collision with

any boundaries. An example of rays is shown in Fig. 2. Since all reflected and transmitted waves from the boundaries ∂D^-, ∂D^+ and ∂M are calculated as plane waves, the displacement $\mathbf{u}^*$ based on the ray theory can be easily obtained as the sum of each plane wave. The detail discussion on the ray theory is referred to Refs. 1 and 2.

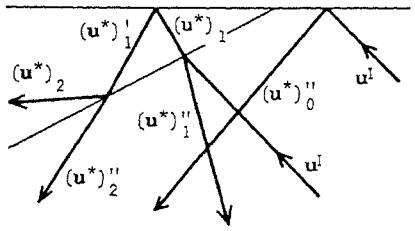

Fig. 2 An example of multiple reflection in a dipping layer (SH wave).

As Ishii and Ellis pointed out, however, the displacement $\mathbf{u}^*$ is not an exact solution for a dipping layer problem and it has several discontinuities along rays propagating without any collisions (for example, $(\mathbf{u}^*)''_0$, $(\mathbf{u}^*)''_1$, $(\mathbf{u}^*)''_2$ and $(\mathbf{u}^*)_2$ in Fig. 2). They also suggested that diffracted waves are generated to cancel discontinuities in the displacement components .

BIE FORMULATION

As mentioned in the previous section, the displacement $\mathbf{u}^*$ obtained by the ray theory has several discontinuities which should be canceled by the diffracted wave field $\mathbf{u}^d$. Here, as shown in Fig. 3, we assume that there exist (N'-1') and (N-1) discontinuities (referred to as discontinuity planes $\partial S_{1'}$, $\partial S_{2'}$,$\cdots$,$\partial S_{N-1'}$ and ∂S_1, ∂S_2,$\cdots$,∂S_{N-1} , respectively) in the domain D^- and D^+, and also assume that the domains D^- and D^+ are divided into N' and N subdomains (referred to as subdomains $D_{1'}$, $D_{2'}$,$\cdots$,$D_{N'}$ and D_1, D_2,$\cdots$,D_N , respectively) by each discontinuity plane.

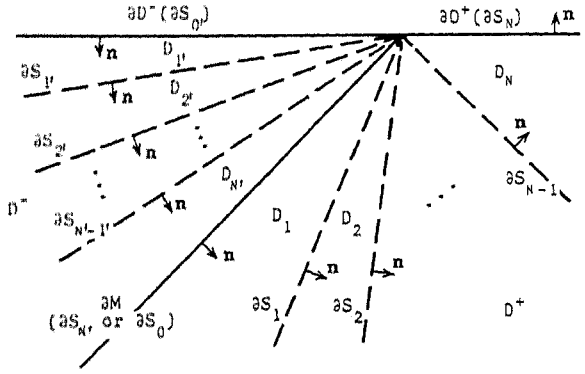

Fig. 3 The subdomains divided by discontinuities based on the ray theory.

First, we consider the BIE formulation in the domain D^+. The total displacement $\mathbf{u}_k$ in D_k are assumed to be expressed as the sum of the computed displacement $\mathbf{u}^*_k$ by the ray theory and the diffracted field $\mathbf{u}^d_k$, i.e.,

$$\mathbf{u}_k=\mathbf{u}^*_k+\mathbf{u}^d_k \quad \text{in } D_k. \tag{11}$$

Since the diffracted wave field $\mathbf{u}^d_k$ satisfies the radiation and regularity

conditions at infinity (Ref. 6), the following integral equations for $\mathbf{u}_k^d$ are obtained from the reciprocal theorem, as follows:

$$-\int_{\partial S_{k-1}}[\mathbf{U}^+(\mathbf{X},\mathbf{y})\mathbf{t}_k^d(\mathbf{y},\omega)-\mathbf{T}^+(\mathbf{X},\mathbf{y})\mathbf{u}_k^d(\mathbf{y},\omega)]dS+\int_{\partial S_k}[\mathbf{U}^+(\mathbf{X},\mathbf{y})\mathbf{t}_k^d(\mathbf{y},\omega)-\mathbf{T}^+(\mathbf{X},\mathbf{y})\mathbf{u}_k^d(\mathbf{y},\omega)]dS$$

$$= \begin{cases} \mathbf{u}_k^d(\mathbf{X},\omega) & \text{in } D_k \qquad (12.a)\\ \mathbf{u}_k^d(\mathbf{x},\omega)/2 & \text{on } \partial S_{k-1} \text{ and } \partial S_k \qquad (k=1,2,\cdots,N) \qquad (12.b)\\ \mathbf{0} & \text{in } (D_k)^c \ [(D_k)^c \text{ denotes the complement of } D_k] \qquad (12.c)\end{cases}$$

where $\mathbf{t}_k^d(\mathbf{y},\omega)\equiv\overset{\mathbf{n}}{\mathbf{T}}(C_L^+,C_T^+,\rho^+;\partial)\mathbf{u}_k^d(\mathbf{y},\omega)$ and $\mathbf{T}^+(\mathbf{X},\mathbf{y})\equiv\mathbf{U}^+(\mathbf{X},\mathbf{y})\overset{\mathbf{n}_y}{\mathbf{T}}(C_L^+,C_T^+,\rho^+;\partial_y)$.
The fundamental solution $\mathbf{U}^+(\mathbf{X},\mathbf{Y})$ in a steady state is well known to have the following form

$$\mathbf{U}^+(\mathbf{X},\mathbf{Y}) = \begin{cases} \frac{i}{4\rho^+C_T^{+2}}[H_0^{(1)}(k_T^+r)\mathbf{1}+\frac{1}{k_T^{+2}}\nabla\nabla(H_0^{(1)}(k_T^+r)-H_0^{(1)}(k_L^+r))] & \\ \qquad\qquad \text{for P-SV problems} & \qquad (13)\\ \frac{i}{4\rho^+C_T^{+2}}H_0^{(1)}(k_T^+r) \qquad\qquad \text{for SH problems} & \qquad (14)\end{cases}$$

where $r=|\mathbf{X}-\mathbf{Y}|$, k_L^+ and k_T^+ are the wave numbers of the longitudinal and the transverse waves in the domain D^+, and $H_0^{(1)}$ is the zeroth order Hankel function of the first kind. If all of N equations (12) are summed up, then we have

$$-\int_{\partial M}[\mathbf{U}^+(\mathbf{X},\mathbf{y})\mathbf{t}_1^d(\mathbf{y},\omega)-\mathbf{T}^+(\mathbf{X},\mathbf{y})\mathbf{u}_1^d(\mathbf{y},\omega)]dS+\int_{\partial D^+}[\mathbf{U}^+(\mathbf{X},\mathbf{y})\mathbf{t}_N^d(\mathbf{y},\omega)-\mathbf{T}^+(\mathbf{X},\mathbf{y})\mathbf{u}_N^d(\mathbf{y},\omega)]dS$$

$$+\sum_{k=1}^{N-1}\int_{\partial S_k}[\mathbf{U}^+(\mathbf{X},\mathbf{y})\{\mathbf{t}_k^d(\mathbf{y},\omega)-\mathbf{t}_{k+1}^d(\mathbf{y},\omega)\}-\mathbf{T}^+(\mathbf{X},\mathbf{y})\{\mathbf{u}_k^d(\mathbf{y},\omega)-\mathbf{u}_{k+1}^d(\mathbf{y},\omega)\}]dS$$

$$= \begin{cases} \mathbf{u}_k^d(\mathbf{X},\omega) & \text{in } D_k \ (k=1,\cdots,N) \qquad (15.a)\\ (\mathbf{u}_k^d(\mathbf{x},\omega)+\mathbf{u}_{k+1}^d(\mathbf{x},\omega))/2 & \text{on } \partial S_k \ (k=1,\cdots,N-1) \qquad (15.b)\\ \mathbf{u}_1^d(\mathbf{x},\omega)/2 \text{ on } \partial M(\partial S_0), \ \mathbf{u}_N^d(\mathbf{x},\omega)/2 \text{ on } \partial D^+(\partial S_N), \ \mathbf{0} & \text{in } (D^+)^c. \qquad (15.c,d,e)\end{cases}$$

Taking account of the continuity conditions on ∂S_k:

$$\mathbf{u}_k=\mathbf{u}_{k+1} \text{ and } \mathbf{t}_k=\mathbf{t}_{k+1} \text{ on } \partial S_k \qquad (16)$$

i.e.,

$$\mathbf{u}_k^d-\mathbf{u}_{k+1}^d=\mathbf{u}_{k+1}^*-\mathbf{u}_k^* \text{ and } \mathbf{t}_k^d-\mathbf{t}_{k+1}^d=\mathbf{t}_{k+1}^*-\mathbf{t}_k^* \text{ on } \partial S_k \qquad (17)$$

and the boundary condition on ∂S_N:

$$\mathbf{t}=\mathbf{0} \text{ on } \partial S_N \qquad (18)$$

i.e.,

$$\mathbf{t}_N^d=\mathbf{0} \text{ on } \partial S_N \ (\text{from } \mathbf{t}_N^*=\mathbf{0} \text{ on } \partial S_N) \qquad (19)$$

equation (15) reduces to the following equation:

$$-\int_{\partial M}[\mathbf{U}^+(\mathbf{X},\mathbf{y})\mathbf{t}_1^d(\mathbf{y},\omega)-\mathbf{T}^+(\mathbf{X},\mathbf{y})\mathbf{u}_1^d(\mathbf{y},\omega)]dS-\int_{\partial D^+}\mathbf{T}^+(\mathbf{X},\mathbf{y})\mathbf{u}_N^d(\mathbf{y},\omega)dS$$

$$+\sum_{k=1}^{N-1}\int_{\partial S_k}[\mathbf{U}^+(\mathbf{X},\mathbf{y})\{\mathbf{t}_{k+1}^*(\mathbf{y},\omega)-\mathbf{t}_k^*(\mathbf{y},\omega)\}-\mathbf{T}^+(\mathbf{X},\mathbf{y})\{\mathbf{u}_{k+1}^*(\mathbf{y},\omega)-\mathbf{u}_k^*(\mathbf{y},\omega)\}]dS$$

$$= \begin{cases} \mathbf{u}_k^d(\mathbf{X},\omega) & \text{in } D_k \ (k=1,\cdots,N) \qquad (20.a)\\ (\mathbf{u}_k^d(\mathbf{x},\omega)+\mathbf{u}_{k+1}^d(\mathbf{x},\omega))/2 & \text{on } \partial S_k \ (k=1,\cdots,N-1) \qquad (20.b)\\ \mathbf{u}_1^d(\mathbf{x},\omega)/2 \text{ on } \partial M(\partial S_0), \ \mathbf{u}_N^d(\mathbf{x},\omega)/2 \text{ on } \partial D^+(\partial S_N), \ \mathbf{0} & \text{in } (D^+)^c. \qquad (20.c,d,e)\end{cases}$$

Similarly, the BIE in the domain D^- is obtained as follows:

$$\int_{\partial D^-}[\mathbf{T}^-(\mathbf{X},\mathbf{y})\mathbf{u}^d_{1'}(\mathbf{y},\omega)dS+\int_{\partial M}[\mathbf{U}^-(\mathbf{X},\mathbf{y})\mathbf{t}^d_{N'}(\mathbf{y},\omega)-\mathbf{T}^-(\mathbf{X},\mathbf{y})\mathbf{u}^d_{N'}(\mathbf{y},\omega)]dS$$

$$+\sum_{k=1'}^{N-1'}\int_{\partial S_{k'}}[\mathbf{U}^-(\mathbf{X},\mathbf{y})\{\mathbf{t}^*_{k+1'}(\mathbf{y},\omega)-\mathbf{t}^*_{k'}(\mathbf{y},\omega)\}-\mathbf{T}^-(\mathbf{X},\mathbf{y})\{\mathbf{u}^*_{k+1'}(\mathbf{y},\omega)-\mathbf{u}^*_{k'}(\mathbf{y},\omega)\}]dS$$

$$=\begin{cases}\mathbf{u}^d_{k'}(\mathbf{X},\omega) & \text{in } D_{k'}\ (k=1',\cdots,N') \qquad (21.a)\\ (\mathbf{u}^d_{k'}(\mathbf{x},\omega)+\mathbf{u}^d_{k+1'}(\mathbf{x},\omega))/2 & \text{on } \partial S_{k'}\ (k=1',\cdots,N-1') \qquad (21.b)\\ \mathbf{u}^d_{1'}(\mathbf{x},\omega)/2 \text{ on } \partial D^-(\partial S_{0'}),\ \mathbf{u}^d_{N'}(\mathbf{x},\omega)/2 & \text{on } \partial M(\partial S_{N'}),\ \mathbf{0} \text{ in } (D^-)^c. \qquad (21.c,d,e)\end{cases}$$

By using the continuity conditions (8) on ∂M:

$$\mathbf{u}^d_{N'}+\mathbf{u}^*_{N'}=\mathbf{u}^d_1+\mathbf{u}^*_1 \quad \text{and} \quad \mathbf{t}^d_{N'}+\mathbf{t}^*_{N'}=\mathbf{t}^d_1+\mathbf{t}^*_1 \quad \text{on } \partial M \qquad (22)$$

i.e.,

$$\mathbf{u}^d_{N'}=\mathbf{u}^d_1 \quad \text{and} \quad \mathbf{t}^d_{N'}=\mathbf{t}^d_1 \quad \text{on } \partial M \ (\text{from } \mathbf{u}^*_{N'}=\mathbf{u}^*_1 \text{ and } \mathbf{t}^*_{N'}=\mathbf{t}^*_1 \text{ on } \partial M) \qquad (23)$$

equations (20) and (21) constitute the coupled BIE with the unknowns $\mathbf{t}^d_1(\mathbf{t}^d_{N'})$, $\mathbf{u}^d_1(\mathbf{u}^d_{N'})$, $\mathbf{u}^d_N$ and $\mathbf{u}^d_{1'}$ on boundaries ∂M, ∂D^+ and ∂D^-. These formulations also provide a theoretical basis to solve the diffracted wave problem in a dipping layer by means of the BIE method.

Equations (20) and (21) were solved numerically to obtain the wave field $\mathbf{u}$ in the domains and on the boundaries. In regard to the numerical procedure employed here, some remarks are described as follows:

(1) Since the diffracted wave field $\mathbf{u}^d$ satisfies the radiation and regularity conditions at infinity, the contribution of the boundary integral along the path far from origin $\mathbf{0}$ is expected to vanish. Therefore, semi-infinite integrals $\int_0^\infty \cdot dS$ on ∂D^-, ∂D^+ and ∂M in equations (20) and (21) were truncated and substituted by finite integrals $\int_0^L \cdot dS$, after evaluating the effective boundary length L so that the truncation error was made sufficiently small.

(2) Semi-infinite integrals on ∂S_k and $\partial S_{k'}$ were evaluated by use of Gaussian and Laguerre numerical integration formulae (Ref. 7).

(3) We paid no special care to the singularity in the traction component at origin $\mathbf{0}$, since it is known that the effect of the singularity on the displacement component is negligible except at the vicinity of origin.

Hitherto, we have discussed the analysis in the steady state, that is, in the frequency domain. Once the displacement $\mathbf{u}(\mathbf{X},\omega)$ in frequency domain is determined, we can obtain the displacement $\mathbf{u}(\mathbf{X},t)$ in time domain by applying the inverse Fourier transform as follows:

$$\mathbf{u}(\mathbf{X},t)=1/(2\pi)\int_{-\infty}^{\infty}\mathbf{u}(\mathbf{X},\omega)\exp(-i\omega t)d\omega. \qquad (24)$$

In this calculation, we employed the fast Fourier transform (FFT). A Ricker wavelet (Ref. 8) was used as an incident pulse .

RESULTS AND DISCUSSION

We show some numerical examples and discuss the effect of diffracted wave on surface ground motions.

Fig. 4 shows one of numerical examples, which is the transient displacement on free surface for an incident SH wave. The parameters in this calculation are as follows: dip angle $\theta_d=45^\circ$, incident angle $\alpha=134^\circ$, velocity ratio $C_T^+/C_T^-=2.0$ and mass density ratio $\rho^+/\rho^-=1.0$. Fig. 4 (a) represents the

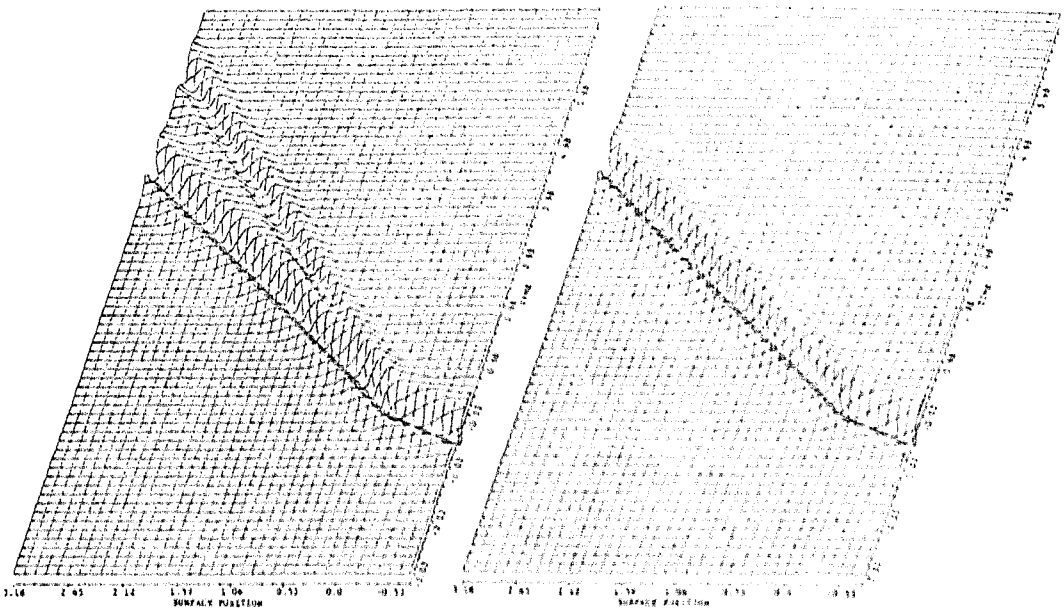

(a) (b)

Fig. 4 The transient displacement on free surface for an incident SH wave for the parameters: $\theta_d=45^o$, $\alpha=134^o$, $C_T^+/C_T^-=2.0$ and $\rho^+/\rho^-=1.0$. ((a) the BIE method and (b) the ray theory)

surface displacement computed by the BIE method, and Fig. 4 (b) by the ray theory. In these figures, the oblique axes denote the normalized time t/t_p, where t_p is referred to the peak period in a Ricker wavelet(Ref. 8), and the abscissas denote the normalized position X_1/λ_p, where λ_p is defined as $\lambda_p=C_T^+t_p$. And Fig. 5 shows the ray diagram corresponding to Fig. 4. In this case, since a large discontinuity (evaluated value=1.33, which is relative to the unit amplitude of incident wave) in the displacement component based on the ray theory exists near the dipping boundary ∂M as shown in Fig.5, it is considered that the refracted wave is induced by the diffracted wave along the discontinuity plane and then propagates with the critical angle $\theta_c=\cos^{-1}(C_T^+/C_T^-)$ from the boundary ∂M into the domain D^- as

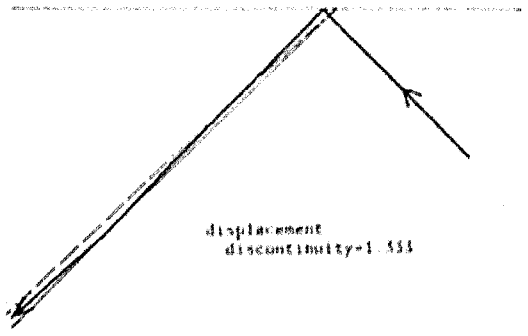

Fig. 5 The ray diagram (solid line) and the discontinuity plane (dashed line) for the same parameters as in Fig. 4.

shown in Fig. 6. Consequently, we conclude that the discrepancy between Fig. 4 (a) and (b) results from the above-mentioned refracted wave.

It is also observed that the diffracted waves have much effect on the displacement on free surface ∂D^-, if a large discontinuity based on the ray theory exists close to the free surface ∂D^-. As an example,

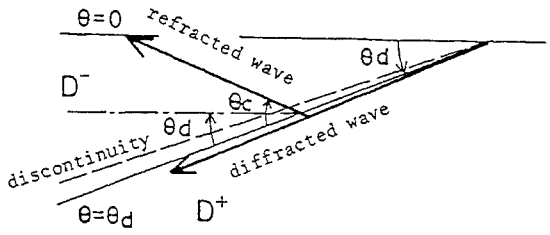

Fig. 6 The refracted wave induced by diffracted wave.

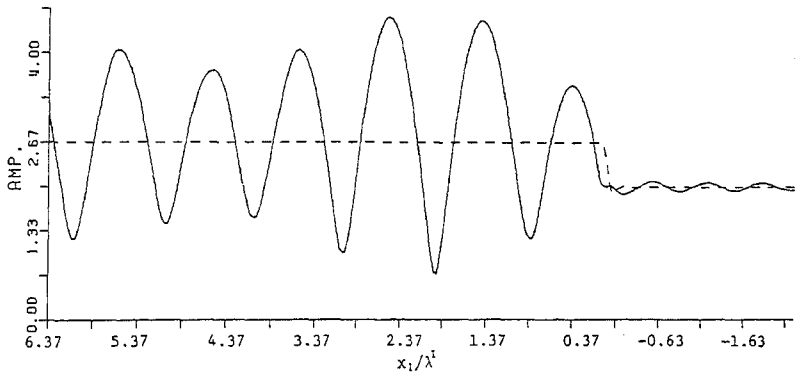

Fig. 7 The amplitude of displacement on the free surface for harmonic incident SH waves. The solid and dashed curves show the result computed by the BIE method and that by the ray theory, respectively. ($\theta_d=30^o$, $\alpha=122^o$, $C_T^+/C_T^-=2.0$ and $\rho^+/\rho^-=1.0$)

the displacement on the free surface for harmonic incident SH wave is shown in Fig. 7, where the solid and dashed curves show the result computed by the BIE method and that by the ray theory, respectively. And its ray diagram is shown in Fig. 8. The parameters used are $\theta_d=30^o$, $\alpha=122^o$, $C_T^+/C_T^-=2.0$ and $\rho^+/\rho^-=1.0$. In Fig. 7, the ordinate shows the amplitude relative to the incident amplitude, and the abscissa shows the normalized position X_1/λ^I, where λ^I denotes the incident wave length. It is found that the difference between solutions obtained by the BIE method and by the ray theory results from the diffracted wave itself along the discontinuity near the

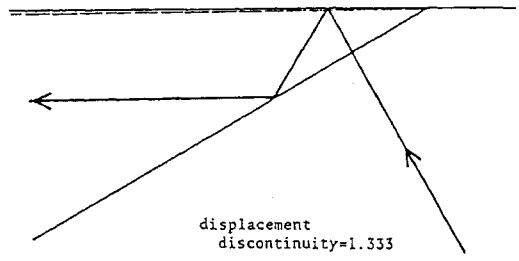

Fig. 8 The ray diagram(solid line) and the discontinuity plane(dashed line) for the same parameters as in Fig. 7.

surface ∂D^-.

From the above two examples (Figs. 4 and 7), it is noted that the surface ground motions are influenced not only by the diffracted waves themselves but also by the refracted waves induced by the diffracted ones.

CONCLUDING REMARKS

The BIE mehtod was employed to analyze the seismic ground motions for a dipping layer. Since the BIE presented in this paper was formulated for diffracted waves, which are excluded in the solution on the basis of the ray theory, a comparison between results obtained by the BIE method and that of the ray theory clarified characteristics of diffracted waves. It was proved from some numerical examples that the diffracted waves played an important role in obtaining the surface ground motions, if a large discontinuity based on the ray theory was located near both boundaries of a dipping layer.

Although numerical examples for SH waves were showed here, a similar discussion can be made easily with respect to P-SV waves problem, where more complex results are obtained due to P-SV mode conversion.

REFERENCES

1. Ishii, H. and R. M. Ellis, "Multiple reflection of plane SH waves by a dipping layer," Bull. Seism. Soc. Am., Vol. 60, 15-28, 1970.

2. Ishii, H. and R. M. Ellis, "Multiple reflection of plane P and SV waves by a dipping layer," Geophy. J. R. astr. Soc., Vol. 20, 11-30, 1970.

3. Aki, K. and P. G. Richards, Quantitative seismology theory and methods, Vol. II, Chap. 13, W. H. Freeman and Company, San Francisco, 1980.

4. Shaw, R. P., "Boundary integral equation methods applied to wave problems," In: Developments in Boundary Element Methods-1, Eds. P. K. Banerjee and R. Butterfield, Applied Science Publishers Ltd, London, 121-153, 1979.

5. Kobayashi, S. and N. Nishimura, "Transient stress analysis of tunnels and caverns of arbitrary shape due to travelling waves," In: Developments in Boundary Element Methods-2, Eds. P. K. Banerjee and R. P. Shaw, Applied Science Publishers Ltd, London, 177-210, 1982.

6. Eringen, A. C. and E. S. Suhubi, Elastodynamics, Vol. 2: Linear Theory, Academic Press, New York, 1975.

7. Niwa, Y. and S. Hirose, "Scattering problems of plane wave in a wedge shaped elastic domain," Proc. 33th Japan Nat. Congr. Appl. Mech., 1983 (in Japanese).

8. Bard, P.-Y. and M. Bouchon, "The seismic response of sediment-filled valleys. Part 1. the case of incident SH waves," Bull. Seism. Soc. Am., Vol. 70, 1263-1286, 1980.